

See discussions, stats, and author profiles for this publication at: <https://www.researchgate.net/publication/347460621>

Energy behavior of Boris algorithm

Article in Chinese Physics B · April 2021

DOI: 10.1088/1674-1056/abd161

CITATIONS

4

READS

181

2 authors, including:



Abdullah Zafar

Chinese Academy of Sciences

18 PUBLICATIONS 27 CITATIONS

[SEE PROFILE](#)

Energy behavior of Boris algorithm

Abdullah Zafar^{1,*} and Majid Khan²

¹*Department of Engineering and Applied Physics,
University of Science and Technology of China, Hefei, Anhui 230026, China*
²*Department of Physics, Quaid-i-Azam University, Islamabad 45320, Pakistan*

Boris numerical scheme due to its long-time stability, accuracy and conservative properties has been widely applied in many studies of magnetized plasmas. Such algorithms conserve the phase space volume and hence provide accurate charge particle orbits. However, this algorithm does not conserve the energy in some special electromagnetic configurations, particularly for long simulation times. Here, we empirically analyze the energy behavior of Boris algorithm by applying it to a 2D autonomous Hamiltonian. The energy behavior of Boris method is found to be strongly related to the integrability of our Hamiltonian system. We have found that if the invariant tori is preserved under Boris discretization, the energy error can be bounded for an exponentially long time, otherwise the said error shows a linear growth. On the contrary, for a non-integrable Hamiltonian system, a random walk pattern has been observed in the energy error.

I. INTRODUCTION

The motion of a non-relativistic particle of charge q and mass m in the electromagnetic fields is governed by Newton's law of motion by taking into account the Lorentz force, i.e. by the following set of equations

$$\frac{dx}{dt} = v, \quad (1)$$

$$\frac{dv}{dt} = \frac{q}{m}(\mathbf{E} + \mathbf{v} \times \mathbf{B}). \quad (2)$$

The discretized form of the above equations for the Boris algorithm can be written as [1–3]

$$\frac{x_{n+1} - x_n}{\Delta t} = v_{n+\frac{1}{2}}, \quad (3)$$

and, respectively

$$\frac{v_{n+\frac{1}{2}} - v_{n-\frac{1}{2}}}{\Delta t} = \frac{q}{m} \left[\mathbf{E}_n + \frac{1}{2} (v_{n+\frac{1}{2}} + v_{n-\frac{1}{2}}) \times \mathbf{B}_n \right], \quad (4)$$

where $\mathbf{E}_n = \mathbf{E}(x_n)$, and $\mathbf{B}_n = \mathbf{B}(x_n)$ are time-independent electric and magnetic field vectors. Despite its simplicity, the Boris algorithm has many advantageous features: it exhibits a long-term accuracy compared to its counterpart, such as the fourth order Runge-Kutta (RK4) method. Moreover, it has been observed that the global error of energy and other conserved quantities, e.g. canonical momentum, can be bounded for all time-steps in the Boris scheme, not to mention the exact energy conservation in the absence of an electric field [3]. Due to these excellent properties, Boris algorithm has been widely used in simulation studies of magnetized plasmas [3–5]. A common misconception about the underlying cause of the long-term fidelity is that the Boris algorithm is a symplectic integrator [6–8]. However, it is actually a volume-preserving method. Further, an earlier study has highlighted that no variational formulation of the Boris algorithm exists, indicating that the long-time stability should be attributed to its volume-preserving characteristics [9–11]. Unlike the symplectic integrator, whose long time energy conservation has been rigorously demonstrated by a backward error analysis [12], the volume-preserving integrator has a little to do with this energy conservation. We refer the reader to the Refs. [2, 13] where one counter-example for which Boris algorithm cannot keep a long time energy conservation and the special conditions under which it can bound these errors. Near-conservation of energy, over long simulation times, has been demonstrated in the conditions where the

* zafar@mail.ustc.edu.cn

magnetic field is constant or the electric potential is quadratic in nature [2]. Nonetheless, the energy behavior of the Boris algorithm in the general cases is not very well understood. This motivates our study to reveal the underlying causes of the different energy behaviors associated with the Boris numerical scheme. The research interests of structure preserving integrators were originated from its qualitative numerical superiority, e.g. conservation of the Kolmogorov-Arnold-Moser (KAM) tori. The near invariant tori of symplectic integrators leads to energy conservation. Similarly, some earlier studies have shown that the invariant torus exists in volume-preserving maps [14, 15]. To be specific, under certain non-degeneracy conditions, any n -dimensional smooth volume-preserving maps close to the integrable ones, preserve a large set of invariant $(n-1)$ -dimensional tori [16]. Thus if the Boris algorithm can preserve the tori, then the conservation of energy would be obtained as a result. Here, we have shown the long time energy behavior of Boris method for a 2-degrees of freedom autonomous Hamiltonian. Numerical experimentation reveals that such an algorithm exhibits several kinds of energy errors. When the invariant tori can be preserved under Boris discretization, the energy error is bounded for an exponentially long time, while if the invariant tori are not preserved, the error exhibit a linear growth. On the other hand, when the Hamiltonian system is non-integrable, Boris algorithm does not conserve energy and exhibits a random walk behavior on the global energy error. For all numerical examples, the symplectic integrator is implemented as a control group for comparisons, which shows a long time energy conservation regardless of whether the original system is integrable or otherwise.

The rest of the article is organized as following: mathematical description of the model is presented in Sec.II. Key results are discussed in Sec.III. Finally, a brief summary of the main results is presented in Sec.IV.

II. MATHEMATICAL DESCRIPTION OF THE MODEL

The specific scheme of Boris algorithm used here is a second-order symmetric version, described by the following set of discretized equations

$$\frac{\mathbf{x}_{n+1} - \mathbf{x}_n}{\Delta t} = \mathbf{v}_{n+\frac{1}{2}}, \quad (5)$$

$$\frac{\mathbf{v}_{n+1} - \mathbf{v}_n}{\Delta t} = \frac{q}{m} \left[\mathbf{E}_n + \frac{1}{2} \left(\mathbf{v}_{n+\frac{1}{2}} + \mathbf{v}_{n-\frac{1}{2}} \right) \times \mathbf{B}_n \right]. \quad (6)$$

We take the implicit Euler method, which is also a second-order symmetric scheme, to write a discretized version of Hamiltonian equations as

$$\frac{\mathbf{q}_{n+1} - \mathbf{q}_n}{\Delta t} = H_p \left(\frac{\mathbf{p}_n + \mathbf{p}_{n+1}}{2}, \frac{\mathbf{q}_n + \mathbf{q}_{n+1}}{2} \right), \quad (7)$$

$$\frac{\mathbf{p}_{n+1} - \mathbf{p}_n}{\Delta t} = -H_q \left(\frac{\mathbf{p}_n + \mathbf{p}_{n+1}}{2}, \frac{\mathbf{q}_n + \mathbf{q}_{n+1}}{2} \right). \quad (8)$$

Here the Hamiltonian for a charged particle in an electromagnetic force field is given by [17]

$$H = \frac{1}{2m} (\mathbf{p} - e\mathbf{A})^2 + e\phi, \quad (9)$$

where all the terms have their usual meaning. We have performed our numerical experiments based on the Hénon-Heiles Hamiltonian system [18], for investigating the invariant tori. The canonical Hénon-Heiles Hamiltonian describes the motion of stars around a galactic center, assuming the motion is restricted to the x - y plane. The corresponding potential can be expressed as [18].

$$\phi(x, y) = \frac{1}{2} (x^2 + y^2) + \lambda \left(x^2 y - \frac{y^3}{3} \right), \quad (10)$$

Here λ is a constant and x, y are coordinates, the motion under this potential can be seen as double harmonic oscillators coupled with the term associated with λ . It has been seen that the third integral exists only for a limited number of initial conditions [18]. In the modern perspective, the initial conditions that do not exhibit a third integral

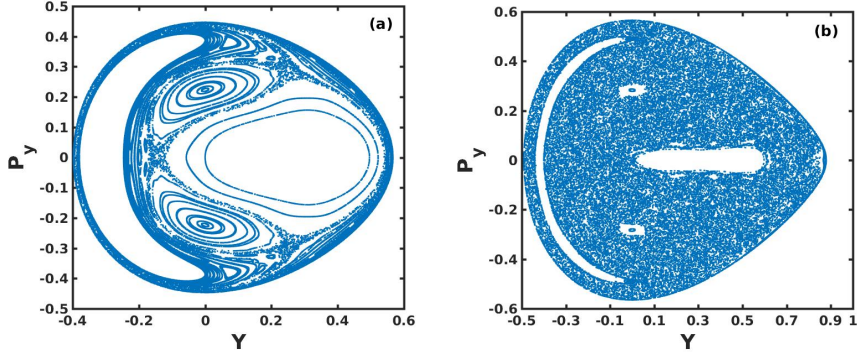


FIG. 1. Poincaré plots of Hénon–Heiles Hamiltonian in (y, P_y) plan, with initial energy (a) 0.1, and (b) 0.16.

of motion is correlated with chaotic orbits. To implement Boris method to a more general case, an extra non-constant magnetic field has also been added. For a constant magnetic field, the one-step map of the Boris algorithm $(\mathbf{x}_n, \mathbf{P}_n) \rightarrow (\mathbf{x}_{n+1}, \mathbf{P}_{n+1})$ is symplectic, where $\mathbf{P}_n = \mathbf{V}_n + e\mathbf{A}_n$. This follows from the fact that the Boris method is a variational integrator if and only if B is a constant [9]. Thus, to investigate the energy behavior of the Boris scheme from its volume-preserving property, without losing any generality, we choose the asymmetric and variable magnetic field as given by

$$B_z = -\frac{B_0}{R_0} \frac{x+y}{2}, \quad (11)$$

with the corresponding vector potential written as

$$\mathbf{A} = \frac{B_0}{4R_0^2} (y^2, -x^2, 0)^\top, \quad (12)$$

On the basis of this system, we can generate various orbits as affected by different initial conditions, which can correspond to integrable and non-integrable regimes. Also, different λ parameters have been used for the construction of the desired Hamiltonian, e.g. $\lambda = 1$ is a regime in which the integrability depends on the initial conditions, while $\lambda = 0$ corresponds to an integrable systems.

Firstly, the phase space behavior of the Hénon–Heiles system has been studied by plotting the Poincaré maps, which is a recurrence plot and can be applied to distinguish chaotic, periodic, or quasi-periodic motions. It focuses only on that regime where the orbit intersects the bottom part of the Poincaré section, instead of studying the motion in the entire phase space. If there are only a few intersection points, then the motion is periodic. If the intersection points constitute a line, the motion is quasi-periodic and if such points are dense and form a random structure, it corresponds to a chaotic regime [19]. In practice, we fix one phase element and plot the other elements each time the selected element has the desired value, thus an intersection surface is obtained. For the Hénon–Heiles Hamiltonian, these plots exhibit various phase space orbits correspond to chaotic and regular motions, with respect to different initial conditions. It is important to note that, in this work, we will use normalized (dimensionless) quantities.

Figure 1 shows the Poincaré maps of the Hénon–Heiles system, and highlights that this system strongly depending on initial conditions can be either integrable or non-integrable. The breaking of the invariant tori can be observed for increasing values of the initial energy, e.g. for $E_0 = 0.16$, the system also exhibits chaotic behavior.

Secondly, the orbit in configuration space can be classified by the means of Fourier transformation, which gives an alternative way to identify the invariant tori [20–22]. For a canonical integrable Hamiltonian system with n degrees of freedom, we can find a canonical transformation, namely from (p, q) to (I, φ) , i.e.

$$I_i = I_i(q_1, \dots, q_n, p_1, \dots, p_n), \quad (13)$$

$$\varphi_i = \varphi_i(q_1, \dots, q_n, p_1, \dots, p_n), \quad (14)$$

where $i = 1, 2, \dots, n$. The transformed coordinates, (I, φ) are called the action-angle variables, which for a special case $H = H(I)$, corresponds to the Hamilton's equations

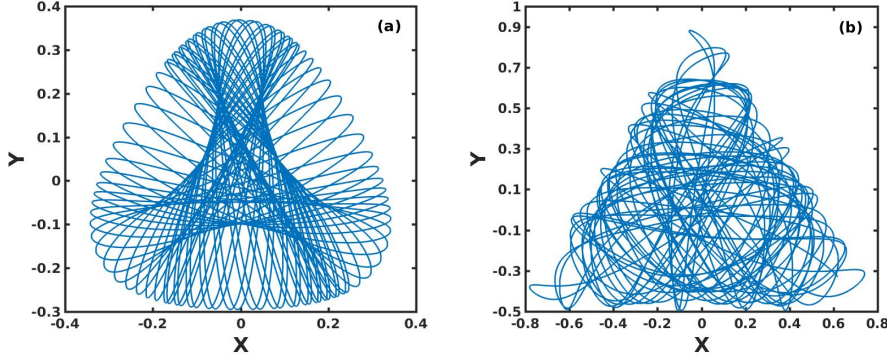


FIG. 2. A regular and chaotic orbit of the Hénon–Heiles system. The initial condition for the regular orbit is (a) $X = [0, 0.1, 0]^\top$, $V = [0.157073238266067, 0.269255830975273, 0]^\top$, while for the chaotic orbit we have (b) $X = [0, 0.1, 0]^\top$ and $V = [0.282596864122024, 0.490039806942659, 0]^\top$.

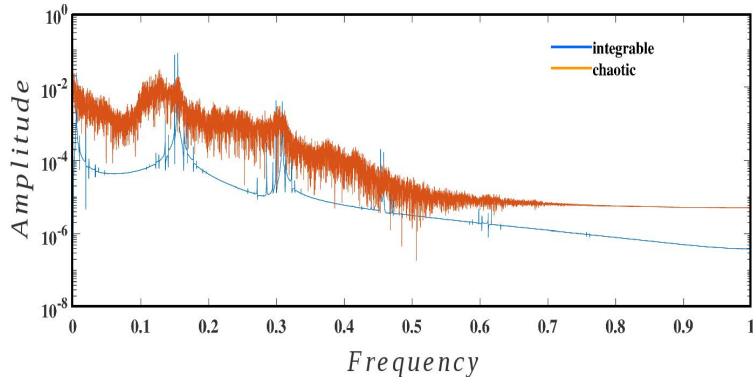


FIG. 3. The DFT spectrum characteristics of orbits for regular and chaotic patterns. The initial conditions are the same as in Fig. 2.

$$\dot{I} = \frac{\partial H(I)}{\partial \varphi} = 0, \quad (15)$$

and

$$\dot{\varphi} = -\frac{\partial H(I)}{\partial I} = \nu(I). \quad (16)$$

The motion on a specific torus has a fundamental frequency and thus a total of n such values for an integrable system, namely $\nu_1, \nu_2, \dots, \nu_n$. Further, the canonical coordinates (q, p) can be expressed as the function of the periodic parameter φ as the Fourier representation, i.e.

$$\mathbf{q}(t) = \sum_{\mathbf{n}} \mathbf{q}_n(I) \cdot e^{i(\mathbf{n} \cdot \nu)t}, \quad (17)$$

where ν is a fundamental frequency vector, and \mathbf{n} is a n -vector with integer components in the interval $[-\infty, +\infty]$. The Fourier coefficients \mathbf{q}_n are functions of the action I [21].

The chaotic and regular orbits corresponding to different initial conditions are shown in Fig. 2, and the Discrete Fourier Transform (DFT) of these orbits is depicted in Fig. 3. As discussed, the spectrum for the integrable system is discrete, whereas for the chaotic motion it exhibits a white noise pattern.

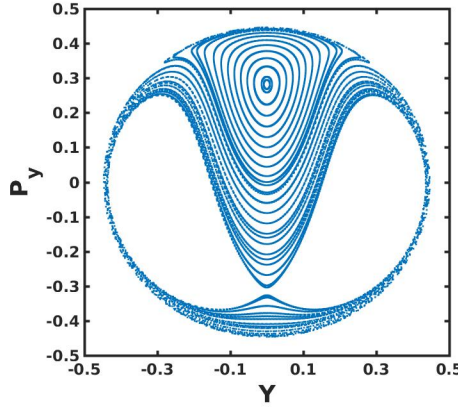


FIG. 4. Poincaré plot of Hénon–Heiles Hamiltonian with the additional asymmetric magnetic field, within the potential parameter $\lambda = 0$. The initial energy is 0.1.

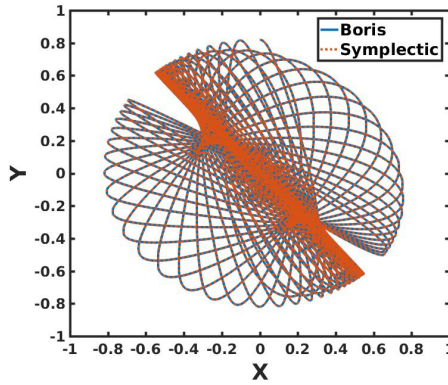


FIG. 5. The orbits of a particle calculated by Boris and symplectic integrators. The initial condition is $X = [0, 0.82, 0]^\top$, $V = [0.123201731589563, 0, 0]^\top$ and the corresponding initial energy is $E_0 = 0.16$, $dt = 0.001$ and $\lambda = 0$.

III. NUMERICAL ANALYSIS AND DISCUSSION

Using the above mentioned scheme, we have investigated the energy error evolution of a single as well as group of statistical charged particles. Moreover, the classification of the orbital type and the correlation of the energy behavior of the Boris algorithm with the system integrability has also been presented. For the demonstration of orbits and energy behavior, we have used the symplectic integrator as a benchmark.

A. Energy behavior under different Hamiltonian regimes

First we set $\lambda = 0$ and plot the consequent phase section in Fig. 4, which exhibit a regular path and the Boris algorithm depicts an excellent long time energy conservation. As for the case when $\lambda = 0$, the harmonic oscillators are decoupled, therefore the KAM structure is not associated with corresponding initial energy. As a consequence, the Poincaré section consists of several concentric closed orbits and is not perturbed by increasing initial energy.

For a given initial conditions $X = [0, 0.82, 0]^\top$, $V = [0.123201731589563, 0, 0]^\top$ and $E_0 = 0.16$, the phase space orbits evaluated by Boris and symplectic algorithms have been illustrated in Fig. 5. In this case, the particle moves along an elliptical orbit while pressing around the counter-diagonal. The motion is quite regular, having several fixed frequencies.

The relative energy errors of Boris and symplectic schemes have also been studied for a long simulation time (about one million iterations) and the findings are depicted in Fig. 6. In this case, both Boris and the symplectic integrators have kept the energy error bounded.

The second example presents a non-integrable Hamiltonian system, i.e. we set $\lambda = 1$, and the computed phase space

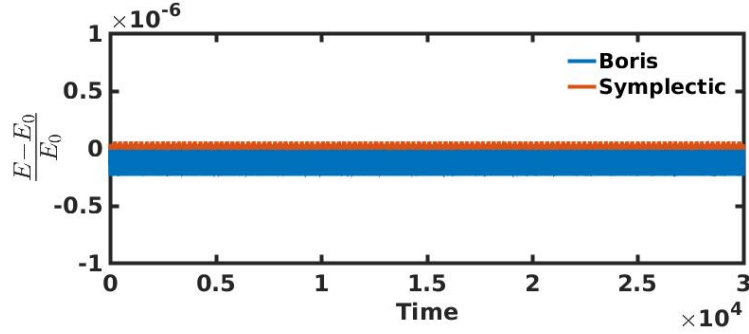


FIG. 6. The evolution of relative error of energy for Boris and symplectic numerical schemes. Initial condition is $X = [0, 0.82, 0]^\top$, $V = [0.123201731589563, 0, 0]^\top$, time interval is $dt = 0.001$, and we iterate over 3×10^7 steps to show the long time behavior of energy error.

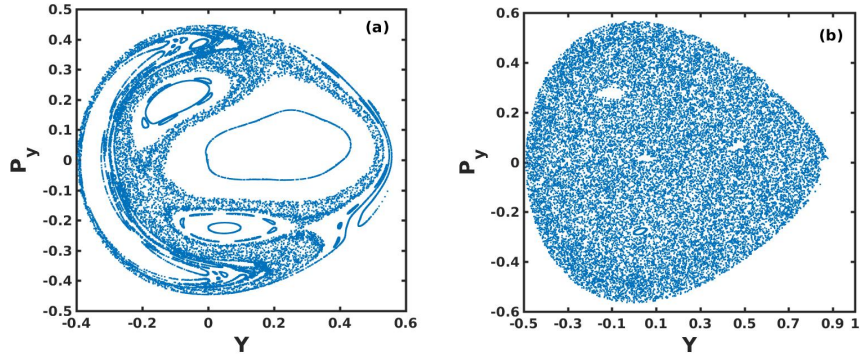


FIG. 7. Poincaré plot of Hénon-Heiles Hamiltonian system with the asymmetric magnetic field. The Poincaré section of the surface lies on the (y, P_y) plane as well, the initial energy in Fig. (a) is 0.1, and Fig. (b) is 0.16.

structure under different initial energies are shown in Fig. 7. After the asymmetric magnetic field is appended, the phase space structure is distorted and becomes complicated. Compared to Fig. 1, for the same energy level $E_0 = 0.1$, more islands among regular concentric circles appears, moreover at even high values, e.g. $E_0 = 0.16$ the entire phase section becomes irregular.

Without losing any generality, we could investigate the energy behavior of Boris algorithm for Hénon-Heiles Hamiltonian. In this regard, the chaotic orbit and corresponding relative energy errors comparison of Boris and symplectic algorithms are shown, respectively in Fig. 8 and Fig. 9. The initial conditions used here are the same as in Fig. 7. The energy error of these chaotic orbits reveals a random walk behavior in particular this error for the Boris stochastically increases with iteration time while symplectic integrator depicts a long term conservation of energy.

To investigate the energy behaviors of Boris algorithm statistically, we consider a group containing 10 particles, all with $E_0 = 0.16$ and are randomly distributed in velocity space. The evolution of the energy error for the entire particle group is shown in Fig. 10. Here one can observe two distinct error responses, namely a “random walk” pattern and “long time conservation” pattern.

Next, we show an example of having the “irregular” orbits and a linear energy error. For that consider the initial energy $E_0 = 0.1$, which corresponds to a regular orbit in the original Hénon-Heiles system. However, with the asymmetric magnetic field, the shape of the orbit turns out to be irregular but not chaotic (the orbit is not sensitive to the initial value). The irregular orbits and their resulting energy behavior of Boris and symplectic integrators are illustrated in Fig. 11 and Fig. 12, respectively. In this case, the energy error of the Boris algorithm exhibits a linear growth pattern, while the energy of the symplectic simulations remains well conserved.

B. Analysis of error growth pattern

In the preceding sections, we have discussed three typical energy trends associated with the Boris scheme. In this regard, the corresponding orbits and the Poincaré sections show a correlation between energy and system integrability.

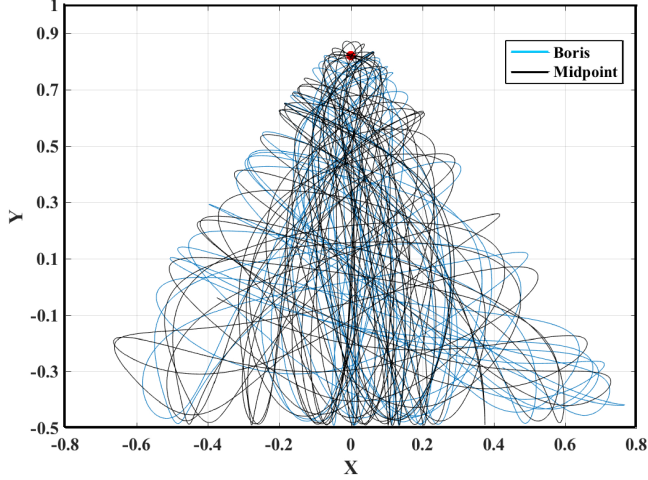


FIG. 8. The orbit in configuration space calculated by Boris algorithm and symplectic integrator. The initial condition is $X = [0, 0.82, 0]^\top$, $V = [0.123201731589563, 0, 0]^\top$, time interval is $dT = 0.001$, and we iterate for 3×10^5 steps. The blue line denotes the result of the Boris algorithm and the black line denotes the result of the symplectic integrator. The red dot is the initial position. In this condition, the orbit exhibits a chaotic pattern.

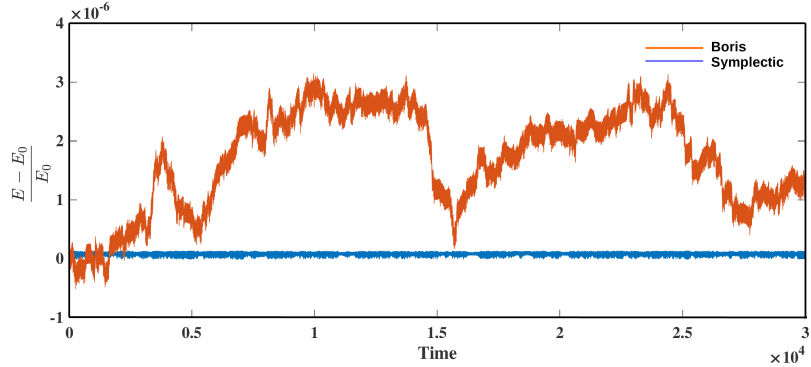


FIG. 9. The evolution of relative error of energy for Boris algorithm and symplectic integrator. The initial condition is $X = [0, 0.82, 0]^\top$, $V = [0.123201731589563, 0, 0]^\top$, time interval is $dT = 0.001$, and we iterate for 3×10^7 steps.

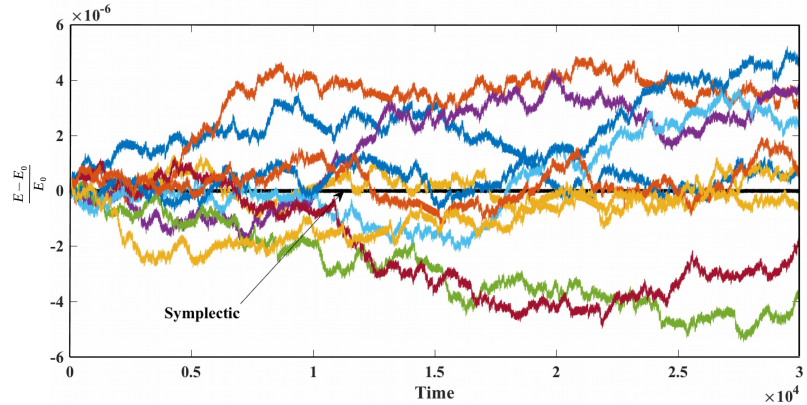


FIG. 10. Energy behavior for a group of 10 particles with the initial energy $E_0 = 0.16$, initial position $X = [0, 0, 0]^\top$, and randomly chosen the sampling points in velocity space. The time interval is $dt = 0.001$ and the calculation steps are 3×10^7 steps for each sampling particle. The black line is the results of the symplectic algorithm. The colored lines denote the results from Boris algorithm.

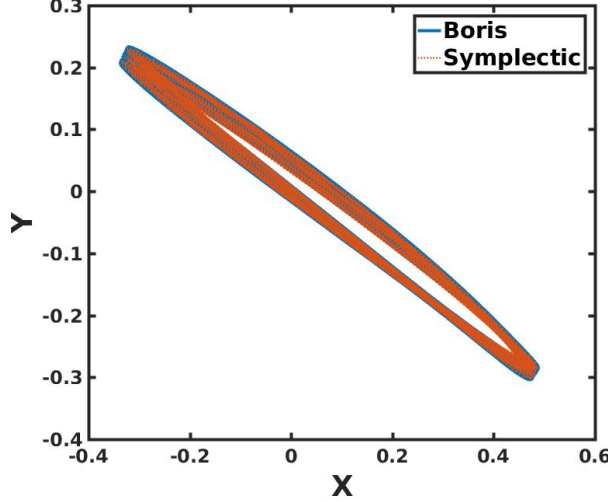


FIG. 11. An irregular orbit calculated by Boris and symplectic integrators. The initial condition is $X = [0, 0, 0]^\top$, $V = [-0.373621484848066, 0.245778327075286, 0]^\top$, $dt = 0.001$ and 3×10^5 steps. The two orbits completely overlap, which means that orbit is not chaotic.

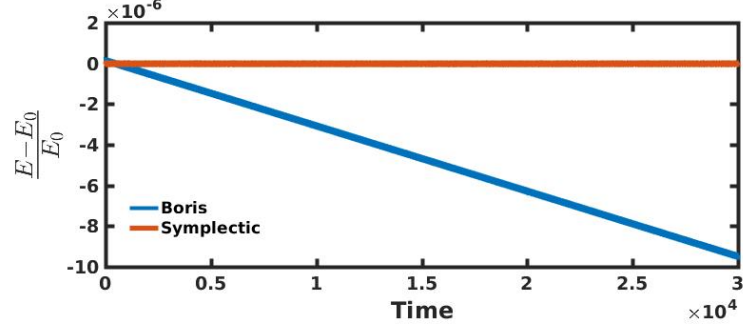


FIG. 12. The evolution of relative energy error for initial condition $X = [0, 0, 0]^\top$, $V = [-0.373621484848066, 0.245778327075286, 0]^\top$, time interval is $dT = 0.001$, and the simulations is performed over 3×10^7 steps to show the long time behavior.

The energy error of the Boris algorithm shows a random walk pattern for particles exhibiting a chaotic motion. However, the causes for the linear-growth in energy error are not well understood. Here some typical cases with such trends have been analyzed, and the results are compared with the corresponding integrable cases. In the following, we will present a brief discussion on the phase sections and the spectrum characteristics of those motions.

We choose an initial point, which corresponds to the regular structure in the Poincaré maps, e.g. as shown in Fig. 7(a). Although this initial condition corresponds to a quasi-periodic motion in which there exists an invariant tori, the Boris algorithm still results in linear growth. The Poincaré plot of a specific particle is shown in Fig. 13.

From Figs. 11 and 13, we can see that the motion is quite regular and quasi-periodic, which means that the invariant tori is existed and Boris algorithm would be able to conserve the energy error for this condition, however it shows a linear growth pattern as depicted in Fig. 12. Actually, the error growth of Boris has originated from the breaking of invariant tori during iterations. To demonstrate this, we apply the DFT to show the information about the invariant tori.

As discussed in Eqs. (13)-(17), the x component of the orbits data is a finite time sequence that are functions of action-angle variables. Thus, a discrete Fourier transformation shows the amplitudes and the frequencies information of the invariant tori. By comparing the spectrum of different orbits, obtained through Boris and symplectic methods, we can quantitatively analyze the evolution of invariant tori, i.e. the energy behavior with respect to KAM structure can be revealed.

To investigate the invariance of tori, the difference of spectrum of orbit sequences for Boris and symplectic schemes are calculated and the results are presented in Fig. 14. The amplitude as evaluated by Boris method is 3 to 4 orders

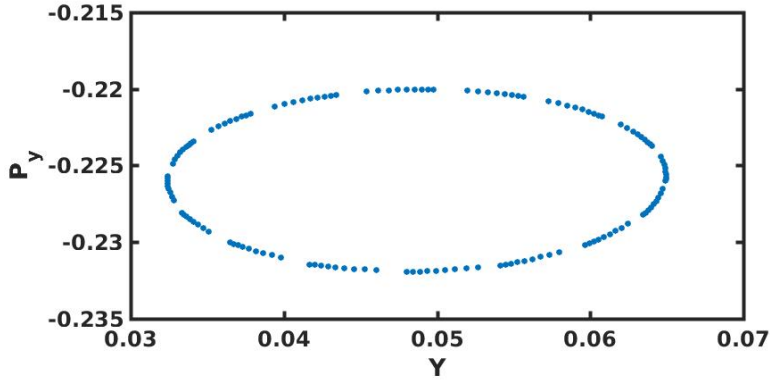


FIG. 13. The Poincaré maps for a particle exhibiting a periodic orbit. The initial energy for this particle is 0.1, and the initial condition is $X = [0, 0, 0]^\top$, $V = [-0.373621484848066, 0.245778327075286, 0]^\top$.

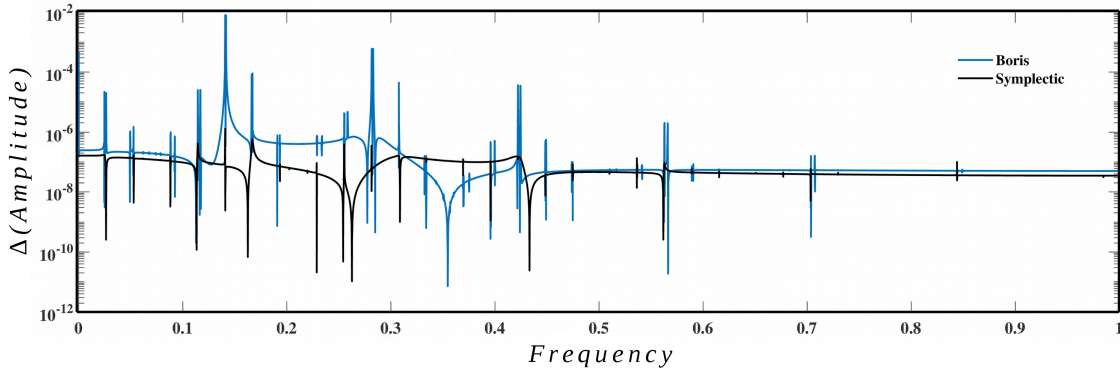


FIG. 14. The difference of spectrum for the two slices of orbit sequences. The blue line denotes the results of Boris while the black line represents symplectic results.

larger than its symplectic counterpart. Thus, for such systems, Boris can not preserve the structure of invariant tori, and for this reason, it exhibits a linear growth in the energy. To further clarify, a complete integrable system has been investigated, with the same initial conditions as in Fig. 5. For which, the Boris algorithm shows a long time energy conservation and the spectrum difference of the orbit in this case is presented in Fig. 15. We observed that the amplitude difference is around 1 – 2 orders smaller than its corresponding case (see Fig. 14). Thus, the invariant tori are preserved under Boris discretization, consequently, the energy error is well behaved.

IV. SUMMARY

To conclude, we have shown various kinds of energy error behaviors of the Boris algorithm for the motion of a charged particle in an electromagnetic field. The energy errors in our numerical examples strongly depend on the integrability of the Hamiltonian. If the Hamiltonian of our system is chaotic, i.e. no invariant tori exists in this case, the energy error of Boris algorithm has a random walk pattern. Whereas, if there is an invariant tori in the original Hamiltonian system, but is not preserved under Boris discretization, the error exhibits a linear growth. As a comparison, the global bound on energy error typically associated with symplectic algorithms still holds for all numerical examples.

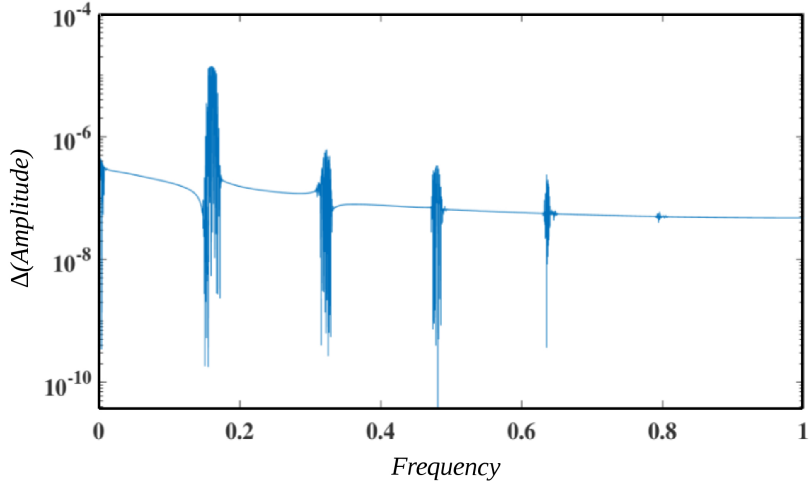


FIG. 15. The characteristic spectrum difference of orbit sequences with simulation time. In this case, The parameter λ in scalar potential is set to be 0.

ACKNOWLEDGEMENTS

The author acknowledges the Chinese Scholarship Council (CSC) to support him as the 2015 CSC awardee (CSC No. 2015GXZQ56). The author would like to thank Dr. Jiangshan Zheng for the technical discussion.

-
- [1] J. P. Boris, in *Proc. Fourth Conf. Num. Sim. Plasmas* (1970) pp. 3–67.
 - [2] E. Hairer and C. Lubich, *BIT Numer. Math* **58**, 969 (2018).
 - [3] H. Qin, S. Zhang, J. Xiao, J. Liu, Y. Sun, and W. M. Tang, *Phys. Plasmas* **20**, 084503 (2013).
 - [4] P. H. Stoltz, J. R. Cary, G. Penn, and J. Wurtele, *PRST-AB* **5**, 094001 (2002).
 - [5] J. Qiang, *Nucl. Instrum. Methods Phys. Res* **867**, 15 (2017).
 - [6] S. D. Webb, *J. Comput. Phys* **270**, 570 (2014).
 - [7] M. Khan, A. Zafar, and M. Kamran, *J. Fusion Energy* **34**, 298 (2015).
 - [8] M. Khan, K. Schoepf, V. Goloborod'Ko, and Z.-M. Sheng, *J. Fusion Energy* **36**, 40 (2017).
 - [9] C. L. Ellison, J. W. Burby, and H. Qin, *J. Comput. Phys* **301**, 489 (2015).
 - [10] M. Khan, M. Khalid, M. Kamran, and R. Khan, *J. Fusion Energy* **39**, 77 (2020).
 - [11] S. Zhang, Y. Jia, and Q. Sun, *J. Comput. Phys* **282**, 43 (2015).
 - [12] E. Hairer, R. I. McLachlan, and R. D. Skeel, *ESAIM: M2AN* **43**, 631 (2009).
 - [13] Y. He, Z. Zhou, Y. Sun, J. Liu, and H. Qin, *Phys. Lett. A* **381**, 568 (2017).
 - [14] A. Gómez and J. D. Meiss, *Chaos* **12**, 289 (2002).
 - [15] C. Q. Cheng and Y. S. Sun, *Celest. Mech. Dyn. Astron* **47**, 275 (1989).
 - [16] Z. Xia, *Ergod. Theory Dyn. Syst* **12**, 621–631 (1992).
 - [17] H. Goldstein, C. Poole, and J. Safko, Classical mechanics. 3rd (2002).
 - [18] M. Henon and C. Heiles, *Astron. J* **69**, 73 (1964).
 - [19] G. Teschl, *Ordinary Differential Equations and Dynamical Systems*, Graduate studies in mathematics (American Mathematical Soc.).
 - [20] E. E. Zotos, *Nonlinear Dyn.* **79**, 1665 (2015).
 - [21] C. Hunter, Spectral analysis of orbits via discrete fourier transforms, in *Observational Manifestation of Chaos in Astrophysical Objects: Invited talks for a workshop held in Moscow, Sternberg Astronomical Institute, 28–29 August 2000*, edited by A. M. Fridman, M. Y. Marov, and R. H. Miller (Springer Netherlands, Dordrecht, 2002) pp. 83–99.
 - [22] G. Voyatzis and S. Ichtiaoglou, *J. Phys. A Math. Theor.* **25**, 5931 (1992).